Indian Journal of Chemical Technology
Vol. 32, September 2025, pp. 632-643
DOI: 10.56042/ijct.v32i5.14716

Synthesis of ternary nanofluids and optimization of their thermophysical properties using artificial neural network

Ganesh Veeraraghavan[1], Pushpavanam Subramaniam[2]* & Mathur Rajesh[1]*

[1]Department of Chemical Engineering, College of Engineering and Technology, SRM Institute of Science and Technology, Kattankulathur, Tamil Nadu-603203, India

[2]Department of Chemical Engineering, Indian Institute of Technology Madras, Chennai, Tamil Nadu-600036, India

*E-mail: spush@iitm.ac.in (PS); rajeshm@srmist.edu.in (MR)

Received 29 October 2024; accepted 17 July 2025

This work focuses primarily on the two-step synthesis of ternary nanofluids consisting of silver (Ag), graphene oxide (GO), and multi-walled carbon nanotubes (MWCNT) in volume fractions ranging from 0.005 to 0.03, their stability and structural (morphological) analysis, and appraisal of their thermophysical properties such as thermal conductivity, viscosity, density and specific heat capacity in the temperature range from 20 to 80°C. The thermal conductivity and viscosity were found to be 0.7845 W/m.K and 0.8718 cP at 30°C for 3 vol %. The work also involved the optimization and validation of these thermophysical parameters using Artificial Neural Network (ANN). The ANN was constituted and tested with the application of Levenberg-Marquardt (LM) algorithm. The titular network size has been inherently optimized as per the relative error to enhance the model's ability to predict thermal conductivity and viscosity. The Levenberg-Marquardt feed-forward network possessing the optimal network design, 6 – 1 (hidden layer nodes – Output layer nodes) for thermal conductivity and 2 – 4 for viscosity have been identified as the best training approach. The ANN results exhibit the coefficient of regression (R^2) to be significant at 0.99736 and 0.99725 for thermal conductivity and viscosity respectively, and the upper limit of relative error was negligible. The same data set subjected to the standard fitting model gave the R^2 of 0.9931 and 0.9944 with mean square error of 0.0064 and 0.0170, respectively.

Keywords: Artificial neural network, Mean square error, Nanofluids, Thermal conductivity, Viscosity

Introduction

Nanofluids are created by dispersing nanoparticles (10–100 nm) in base fluids, enhancing thermophysical and morphological properties. These improvements enable wide-ranging applications across energy transfer, materials science, petroleum drilling, and emerging fields like biomedical drug delivery[1,2]. Commonly used particles include metals, metal oxides, and carbon allotropes due to their superior thermal properties[3,4]. Nanofluids are synthesized via two main methods: the one-step (single-pot) method, where nanoparticles form directly within the base fluid, and the two-step method, where nanoparticles are produced separately and then dispersed. Each method has trade-offs in particle size, purity, stability, scalability, and cost[5]. Typically, the one-step method limits nanoparticle volume concentration compared to the two-step approach. Carbon nanotubes (CNTs), due to their high thermal conductivity, unique structure, and exceptional electrical, optical, and mechanical properties, are a preferred nanomaterial for enhancing nanofluid performance[6].

Keblinski *et al*. synthesized nanoparticles via chemical vapour condensation and dispersed them in fluids to create nanofluids[7]. Ahmed *et al*. prepared a ternary hybrid nanofluid (ZnO-Al_2O_3-TiO_2/DW) using two-hour probe sonication, finding that 0.1 wt% showed the best stability and lowest sedimentation[8]. Mousavi *et al*. synthesized a CuO-MgO-TiO_2/water ternary hybrid nanofluid via thermochemical methods[9]. Babita *et al*. prepared CNT/water nanofluids using a two-step process and varying surfactant/CNT ratios, achieving high Zeta potential values[10].

The performance of nanofluids relies on their stability, specifically, the ability of nanoparticles to remain uniformly dispersed without agglomeration or settling. Stability significantly affects thermo-fluid properties, making it critical for industrial applications. Methods to evaluate nanofluid stability include visual inspection, sedimentation analysis, Zeta potential measurement, and dynamic light scattering (DLS). Brownian motion is key to nanofluid stability, measured via Zeta potential, which reflects diffuse

layer charges. Higher system entropy from Brownian motion enhances thermal properties. According to DLVO theory (Derjaguin, Landau, Verwey, and Overbeek Theory), stability balances van der Waals attractions and electric double layer (EDL) repulsion[11].

Xian *et al*. found that mono nanofluids had higher zeta potential and stability than hybrids; zeta potential increased linearly with optimal sonication time (60 min for mono, 120 min for hybrids) but declined after that[12]. Innovations like using Artificial Neural Networks (ANN) and Adaptive Neuro Fuzzy Inference Systems (ANFIS) for property modeling are also advancing the field[13,14].

ANNs mimic the human brain, excelling at pattern recognition, training, and self-awareness, the key for deep learning. They are pivotal in research and AI development, featuring human-like functionality, machine learning, adaptability, data analysis, predictive modeling, and automation. With the growth of machine learning, key approaches include ANN, Convolutional Neural Networks (CNN), and Response Surface Methodology (RSM), each with unique strengths[15]. ANN, used in various scientific and engineering fields, excels in pattern recognition, non-linear modeling, adaptability, feature extraction, and prediction. However, proper data selection, validation, and interpretation remain crucial for meaningful results.

ANN techniques, especially the Multi-Layer Perceptron (MLP) network, are commonly used for solving non-linear regression problems. MLP typically includes input, hidden, and output layers[16]. Neural Network Training (NNT) involves determining weights and biases to model relationships between inputs and targets. Success depends on selecting relevant inputs and following steps like data acquisition, model selection, and testing with new data. Multi-Layer Perceptrons (MLPs) include one or more hidden layers with neurons that link inputs to outputs, enabling the capture of complex relationships. The optimal number of hidden neurons is determined through testing. The Levenberg–Marquardt algorithm, a faster alternative to gradient descent, is used to optimize MLPs[17].

The Levenberg-Marquardt (LM) algorithm blends gradient descent and Gauss-Newton methods to efficiently minimize non-linear least squares problems in ANN training[18-20]. Its key features include faster convergence without oscillations, the use of second-order error surface information, and a regularization term to prevent overfitting. LM is versatile and suitable for training various ANN types across regression, classification, and time-series tasks. ANNs are widely used to model and predict nanofluid properties such as thermal conductivity, viscosity, specific heat, nanoparticle stability, and multi-objective optimizations[21]. The accuracy of ANN models depends on quality training data and requires experimental validation. Training involves using data for model building, validation for hyperparameter tuning, and testing to assess performance on unseen data.

Zhao *et al*. found that using nanoparticle cluster average size as input improved thermal conductivity predictions over a 3-input model[22]. The Levenberg-Marquardt Backpropagation algorithm enhanced ANN model efficiency[23]. Balaji *et al*. used ANN to predict the thermal properties of MWCNT nanofluids with a 65:25:10 split for training, testing, and validation[24]. Dehkordi *et al*. applied feed-forward ANN to study thermal conductivity of graphene and tungsten oxide nanofluids in paraffin by varying mass fraction and temperature[25]. Tian *et al*. employed the trainbr ANN algorithm and feed-forward perceptron to model the thermal conductivity of graphene oxide-Al_2O_3/Water-EG hybrid nanofluids[26]. Adun *et al*. studied ternary hybrid nanofluids (Al_2O_3, ZnO, Fe_3O_4) at 25–65°C using Gaussian Process Regression, achieving R^2 of 0.97 for thermal conductivity and 0.93 for viscosity[27]. Ji *et al*. applied ANN to analyze nanofluid stability, highlighting sonication time as a key factor[28]. MgO/water nanofluid properties, heat transfer coefficient, thermal efficiency, and friction factor, were predicted using Levenberg-Marquardt ANN, outperforming correlation methods[29].

The objective of this work is to synthesize hybrid (ternary) nanofluid through the two-step process, characterize their morphology and stability, estimate their thermophysical properties, and optimize the properties with ANN using the Levenberg-Marquardt algorithm.

Experimental Section

Preparation of constituent nanoparticles

The necessary chemicals were procured from Sigma Aldrich and standard procedures were followed with regard to the usage of DI water, reagents, solvents, and handling of glass wares along with the mixing protocols. Also, proper safety aspects

were followed as warranted by this work. The ternary hybrid nanofluids were prepared using MWCNT, GO, and silver nanoparticles, either synthesized or activated. Silver nanoparticles were synthesized by the reduction of $AgNO_3$ using $NaBH_4$ followed by centrifugation and controlled drying[30].

Graphene oxide nanoparticles were synthesized from Graphite flakes by employing the modified Hummer's method[31,32]. The resultant solution is centrifuged and the gel-like residue is subjected to vacuum drying at 60°C for more than 6 h to obtain the Graphene oxide powder. Since carbon nanotubes (CNTs) are hydrophobic to polar solvents and insoluble in water, functionalizing them is essential to enable bonding with water and ensure uniform dispersion. To achieve this, multi-walled carbon nanotubes (MWCNTs) were functionalized using a 3:1 acid solution of sulfuric acid (H_2SO_4) and nitric acid (HNO_3), followed by a series of dilutions and drying steps to complete the process[33].

The above synthesized/functionalized nanoparticles are dispersed in DI water and subjected to intensive sonication for 120 min and are mixed in the desired ratio to form various concentrations of nanocomponent by volume, φ, as defined in Eq. (1)[5] to form five different desired volume fractions of 0.005, 0.01, 0.015, 0.02 and 0.03. To aid the stability, each sample is subjected to probe sonication and this solution is treated as the ternary (hybrid) nanofluid and is subjected to characterizations.

$$\varphi = \frac{\sum_{i=1}^{3}\left(\frac{m}{\rho}\right)_{np,i}}{\sum_{i=1}^{3}\left(\frac{m}{\rho}\right)_{np,i}+\left(\frac{m}{\rho}\right)_{water}} \quad \ldots (1)$$

where m = mass of constituent species, ρ = density of constituent species.

Thermophysical properties

Estimation of thermophysical properties of nanofluids involves understanding how the presence of nanoparticles influences parameters like thermal conductivity, viscosity, and heat capacity. The Effective Thermal Conductivity is validated against the measured values using the composite model - Maxwell's model or the Bruggeman model and empirical correlations.

The viscosity of the resultant ternary nanofluid is measured and validated against the established Einstein's Model and correlations, which relate factors such as volume fraction, temperature, and shear rate. Other than the thermal conductivity and viscosity, specific heat capacity and density are the other parameters measured.

The experimental validation of nanofluid properties is crucial, and hence the choice of models or correlations is critical and often involves a trade-off between simplicity and accuracy. The key thermal property of thermal conductivity was studied using KD2 Pro Analyzer (Decagon Devises, US) and the fluid absolute viscosity was measured using the research standard Brookfield viscometer. The density of the ternary nanofluid is analyzed by the Anton Paar density meter and the specific heat capacity using the Differential Scanning Calorimeter (DSC), NETZSCH, Germany.

Morphological Analysis

The characterization and morphological evaluation of ternary nanofluids involve a combination of techniques to assess the composition, structure, and distribution of nanoparticles.

XRD Analysis

X-ray diffraction (XRD) analysis was done using BRUKER D8 Advance, Davinci analyzer system (USA). XRD is used to determine whether a sample is crystalline or amorphous by measuring X-ray scattering angles and intensities. In crystalline structures, constructive interference of X-rays occurs due to repetitive atomic arrangements, producing characteristic diffraction peaks. Each peak corresponds to specific scattering angles, revealing the structural identity of the sample's components.

Scanning Electron Microscopy (SEM) analysis

Thermo Scientific Apreo high-resolution Scanning Electron Microscope (HRSEM) was used to determine the surface topology and species composition of the CNF. SEM images a sample by scanning it with a high-energy electron beam in a raster pattern. Emitted via thermionic or field emission, the beam passes through electromagnetic lenses and interacts with the sample surface, producing signals like secondary electrons, backscattered electrons, and X-rays. Nanofluid samples are coated with a conductive layer and analyzed to reveal surface morphology, particle aggregation, and distribution.

Transmission Electron Microscopy (TEM) analysis

High-Resolution Transmission Electron Microscopy (JEOL JEM 2100 Plus, Japan) was used to study the crystal structure of the Ag-GO-CNT composite. This technique reveals lattice fringes and near-atomic resolution images, enabling analysis of crystalline defects, interfaces, multilayers, and nanostructures. Nanofluid samples were deposited on a TEM grid, and electrons transmitted through the sample produced detailed images showing particle size, morphology, and distribution at the nanoscale.

Stability analysis

Zeta potential is the electric potential at the Stern layer in colloids and nanofluids, reflecting particle charge and stability. It affects electrophoretic mobility and Brownian motion. The Dynamic Light Scattering (DLS) technique measures zeta potential and particle size distribution by analyzing the scattering of monochromatic light. The auto-correlation function of the scattered light helps determine the decay constant and wave vector, indicating particle dynamics and stability. By this, the translational diffusion coefficient (D_{trans}) can be known. The Stokes-Einstein equation[11] given below (Eq. 2) relates the diffusion coefficient to the diameter of the particles.

$$D_h = \frac{k_B T}{3\pi\eta D_{trans}} \quad \ldots (2)$$

where, k_B denotes the Boltzmann constant, T denotes temperature, η denotes the viscosity, D_{trans} denotes the translational diffusion coefficient, and D_h denotes the hydrodynamic diameter of the particle. This equation is characteristically used to detail the particle size distribution for various values of D_{trans} as well as the zeta potential which is dependent on electrophoretic mobility. The Malvern Nano ZS-90 is used to evaluate the surface charge and stability of nanoparticles in the nanofluid by analyzing the electrophoretic mobility of nanoparticles in the presence of an electric field, thereby shedding information on the stability and potential for aggregation.

Artificial Neural Network

The current work applies the ANN in the following manner:

i. Extraction of experimental data
ii. Proposal of Algorithm to evaluate the best neuron number (in the hidden layer)
iii. Comparison of the results with the ANN outputs.

The objective of this ANN study is to train, test, and predict the fluid-thermal properties based on the volume fraction (φ) and temperature (T) as inputs. Since the output values of ANN are impacted by neuron number, an algorithmic rule is introduced to determine the best neuron number, wherein different neuron numbers are evaluated and their performances stored, and sorted based on the same. The total number of data points forms a matrix of concentration vs. temperature data for both thermal conductivity and viscosity. These data points are divided into three categories: training, validation, and testing. Specifically, 80% of the observations are allocated for training, 10% for validation, and the remaining 10% for testing.

The ANN structure used in this work is depicted in Fig. 1. As per traditional methods, three layers: Input, Hidden, and output form the construction of the neural network and the transfer functions used are the sigmoid (exponential and tangential) and linear.

For the hidden layer, the Hyperbolic tangential sigmoid forms the activation function. To incorporate a degree of independence, the bias function is induced, which makes the networks more effective than unbiased ones. The weighted sum of the j^{th} neuron (N_j), is given by Eq. (3)[34],

$$N_j = \sum_{i=1}^{n} x_i w_{ij} + b_i \quad \ldots (3)$$

where, x_i is the i^{th} neuron output, w_{ij} gives the interaction between the i^{th} and j^{th} neuron and b_i represent the quantified bias induced.

The mainstay statistical parameters used to evaluate the efficacy of a chosen neural network model, namely the mean squared error (MSE) and coefficient of regression (R^2) are given in Eq. (4) and Eq. (5) respectively[34,35].

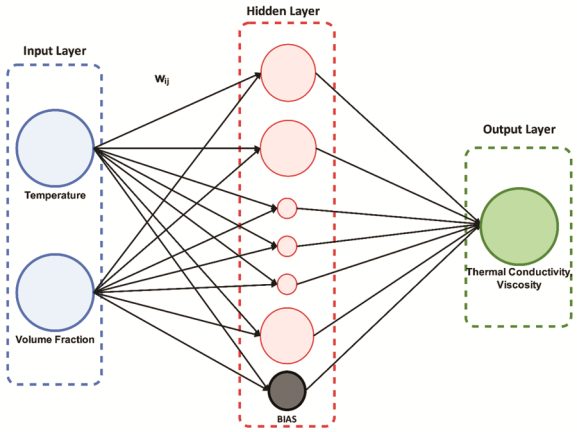

Fig. 1 — Overview of Neural Network used in this work

$$\text{MSE} = \frac{1}{n}\sum_{i=1}^{n}(y_e - y_i)^2 \quad \ldots(4)$$

where y_e and y_i are experimental (actual) and predicted responses, respectively.

$$R^2 = 1 - \frac{\sum_{i=1}^{n}(xi^{\exp} - xi^{pred})^2}{\sum_{i=1}^{n}(xi^{\exp} - x^{\exp})^2} \quad \ldots(5)$$

R^2 represents the niche of fit for the chosen model and is the extent of correlation between the factual and the predicted output.

Results and Discussion

Nanofluid characterization

As discussed above, the synthesized nanofluid is subjected to characterization studies for its morphology, stability, and thermophysical property estimation. The results of the same are discussed below.

Morphological analysis

The XRD peak analysis for the sample is given in Fig. 2. The presence of characteristic peak of silver at 38° could be seen along with the carbon peaks.

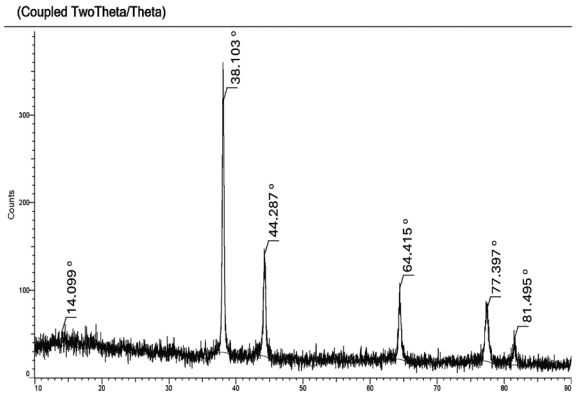

Fig. 2 — XRD Spectrum of the ternary nanofluid

The shape of the peaks confirms the amorphous nature of the nanoparticles. The XRD peaks at 38.103°, 64.415°, and 77.397° correspond to 111, 220, and 311 planes for silver, respectively, whereas the peaks around 14.1° correspond to GO and around 44.287° that of CNT[30,36].

The HRSEM micrographs showed sheet-like morphology of graphene oxide, interlayers of spherical silver particles, and the rod-shaped CNT. Fig. 3 depicts the SEM micrograph for the sample at 25000x. The characteristic cylindrical CNTs and the exfoliated plate-like structured GO are visible along with the presence of silver. The EDS of the SEM analysis confirms the same.

The ternary nanofluid synthesized above is cast on the TEM grid and is magnified at varied scales upto 50000x. From the TEM image (Fig. 4), it is observed that the spherical silver nanoparticles of size around 60 – 100 nm are embedded over the layers of exfoliated sheets of graphene oxide with the cylindrical CNT interwoven. The same is reinforced through the EDX spectrum.

Stability analysis

The DLS results (Fig. 5) show the stability of the ternary hybrid nanofluid after 20 days. The zeta potential recorded for the sample at around -29 mV is bordering on the good stability regime, especially after 20-day period. Though several concentrations upto 5 vol % were prepared and tested for stability, only concentrations upto 3 vol % were found to be stable, with higher concentrations undergoing slow to rapid settling with an increase in concentrations.

Property estimation

Since the intended nature of this work is to apply the synthesized nanofluids for heat transfer application, the thermophysical properties of the same were studied in detail using the techniques mentioned above.

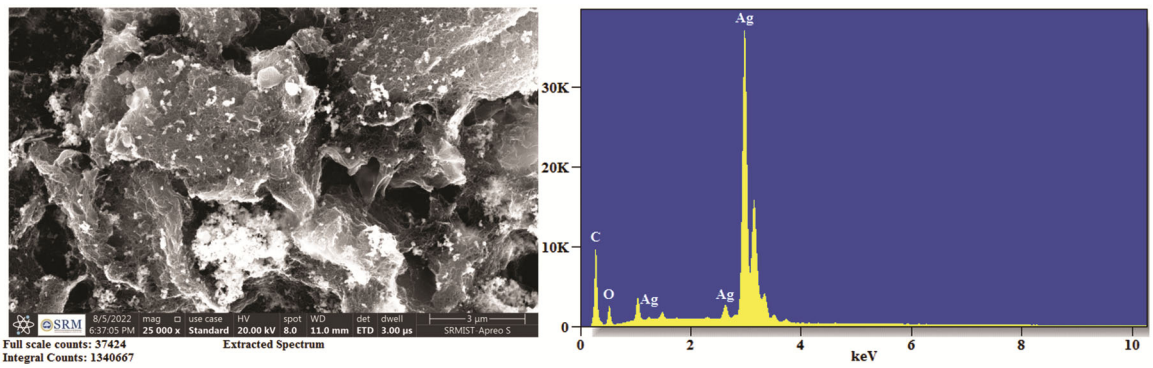

Fig. 3 — SEM micrograph of ternary nanofluid at 25000x and EDS

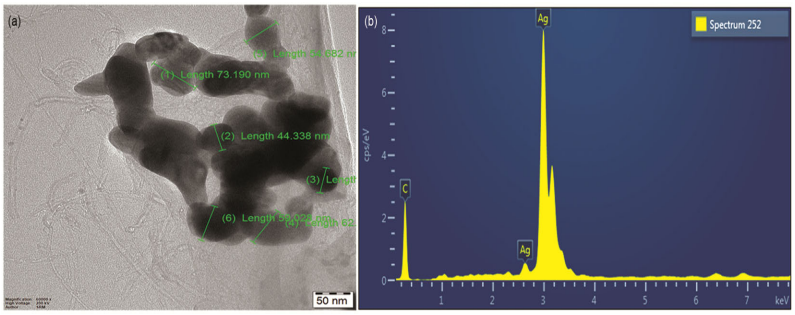

Fig. 4 — TEM image and EDX of ternary nanofluid

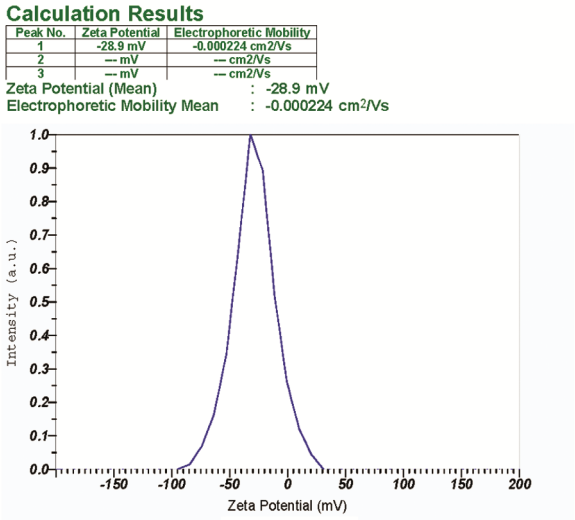

Fig. 5 — Zeta Potential of the 3 vol% ternary nanofluid after 20 days

The mentioned properties of the nanofluid at different temperatures were measured and compared against the standard correlation for properties[37-39]. The measured properties of the 3 vol % ternary nanofluid are tabulated in Table 1.

The core thermal property viz. thermal conductivity of the ternary nanofluid measured at different solid concentrations and temperatures are plotted in Fig. 6(a), whereas the thermal conductivity ratio (i.e.) the ratio of the thermal conductivity of ternary nanofluid to that of the base fluid at that temperature is plotted in Fig. 6(b). The thermal conductivity of the nanofluid increases with increased solid load, as well as with increasing temperatures. The 3 vol% nanofluid exhibited a maximum thermal conductivity ratio of around 1.34 (34% enhancement at 80°C, whereas the same ratio was around 1.31 (31 % enhancement) at the practical exposure temperature of 40 - 50°C. Similarly, the other significant thermal flow property viz. viscosity of the ternary nanofluid at various concentrations and temperatures are plotted in Fig. 6(c). As can be seen, the fluid viscosity increases with increased solid concentrations, while the same decreases with increasing temperature. This trend is expected because of the similar temperature dependency of the base fluid, water. As the desired viscosity of the fluid should be less, the nanofluids at higher concentrations are not viable for application because of their higher viscosity. The other properties like specific heat capacity and density are also studied and the results are tabulated in Table 1.

Table 1 — Estimated thermophysical properties of 3 vol % Ternary Nanofluid

Temperature (°C)	Thermal conductivity (W/m.K)	Viscosity (cP)	Sp. heat capacity (J/g.K)	Density (g/cc)
20	0.7622	1.0881	3.9761	1.0193
30	0.7845	0.8718	3.9601	1.0189
40	0.8210	0.7204	3.9610	1.0178
50	0.8465	0.6054	3.9742	1.0135
60	0.8701	0.5224	3.9861	1.0102
70	0.8794	0.4501	3.9967	1.0084
80	0.8983	0.4014	4.0020	0.9997

ANN results

In this work, the properties that signify the thermal behavior of nanofluids, thermal conductivity, and viscosity are subjected to MLP networks, and the analyzed results are presented in detail. Various valid concentrations of 0.5, 1.0, 1.5, 2.0, and 3.0 volume % solid and the temperatures in the range of 20 - 80°C were selected as model input values for patterning the thermal conductivity along with viscosity of the CNT-GO-Ag in water hybrid nanofluid using the MLP network. In this study, R_{Train}, R_{Val}, R_{Test}, and $R_{Overall}$ represent the correlation coefficient of the interactions between the yield model (YM) and the training dataset, validation data, testing set; and overall experimental data, respectively. Since the dataset is limited, the proportion of training, validation, and testing dataset is maintained as 80:10:10. The most

conditioned models for the two desired parameters are identified based on the mean square error (MSE) values, obtained from the performance graph of each run, with the established rule being the network layers exhibiting the minimal Mean Square Error (MSE) are validated to be the optimal network structure[20,29,40].

The performance results of ANN with different number of neurons, for testing data in a unitary and double hidden layer setup, groomed with the Levenberg-Marquardt (LM) rule for nanofluids is shown in Table 2 (thermal conductivity) and Table 3 (viscosity). The results are sorted based on the neuron

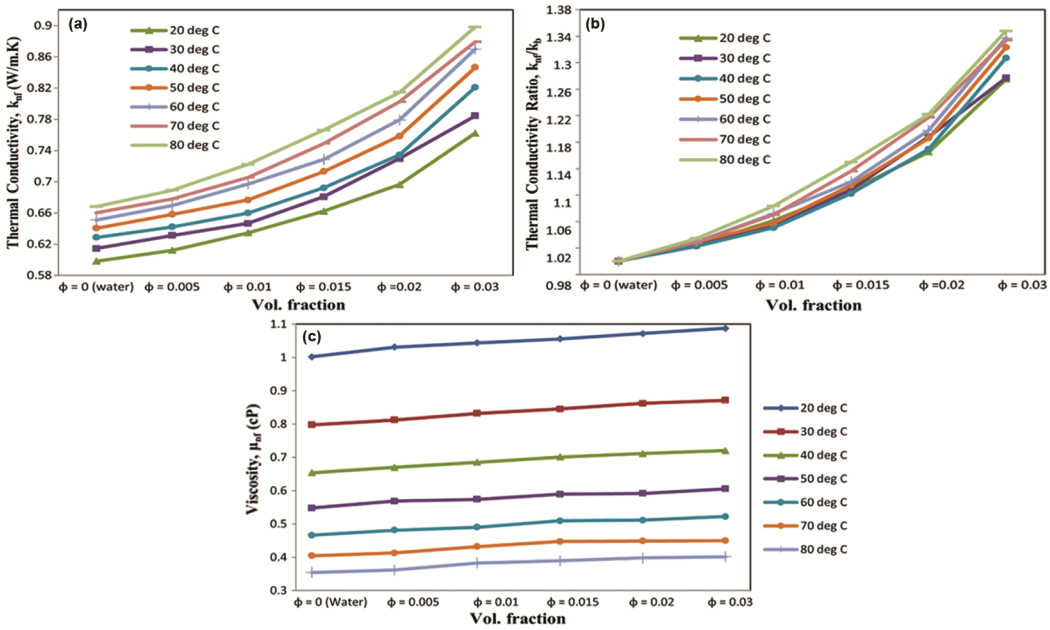

Fig. 6 — Variation of properties at different temperatures: (a) k vs volume fraction, (b) k_{ratio} vs volume fraction and (c) viscosity of nanofluids vs volume fraction

Table 2 — Optimal network estimation for Thermal conductivity of ternary nanofluid

No. of hidden layers	No. of neurons in each hidden layer	R for TRAIN data (R_{train})	R for VALIDATION data (R_{val})	R for TEST data (R_{test})	R for ALL data ($R_{overall}$)	Mean Square Error (MSE)
1	2	0.99998	0.98999	0.99996	0.98992	2.91E-10
1	3	0.97686	0.98949	0.95522	0.98190	2.27E-08
1	4	0.99484	0.99180	0.98522	0.99418	6.44E-09
1	5	0.98261	0.99905	0.99786	0.98905	1.59E-09
1	6	0.98312	0.95407	0.83288	0.97681	3.19E-08
1	7	0.99762	0.99590	0.93543	0.97463	2.91E-08
1	8	0.99929	0.99967	0.99841	0.99709	3.46E-10
1	9	0.99926	0.99958	0.99839	0.99865	2.09E-09
1	10	0.95881	0.98753	0.98190	0.96268	3.72E-08
1	20	0.96031	0.79981	0.81784	0.90920	6.70E-08
2	2	0.99347	0.99689	0.99338	0.99449	6.50E-09
2	3	0.96669	0.94463	0.98208	0.95798	5.20E-08
2	4	0.98206	0.98152	0.99419	0.98176	8.10E-09
2	5	0.98336	0.97827	0.99681	0.97794	4.37E-08
2	6	0.99936	0.99983	0.99980	0.99949	1.37E-10
2	7	0.99844	0.99709	0.99914	0.99836	1.05E-09
2	8	0.94993	0.99061	0.92495	0.94467	4.18E-08
2	9	0.99671	0.85436	0.93071	0.95851	1.40E-07
2	10	0.99851	0.99788	0.99806	0.99633	2.16E-09
2	20	0.99567	0.74834	0.93787	0.92045	2.27E-07

Table 3 — Optimal network estimation for Viscosity of ternary nanofluid

No. of hidden layers	No. of neurons in each hidden layer	R for TRAIN data (R_{train})	R for VALIDATION data (R_{val})	R for TEST data (R_{test})	R for ALL data ($R_{overall}$)	Mean Square Error (MSE)
1	2	0.99845	0.99947	0.99968	0.99833	1.26E-09
1	3	0.94225	0.93865	0.95041	0.94131	4.54E-08
1	4	0.95714	0.99807	0.93891	0.95290	3.84E-08
1	5	0.97817	0.98668	0.99475	0.97934	1.13E-08
1	6	0.97951	0.93361	0.97808	0.97717	2.56E-08
1	7	0.99761	0.99934	0.97947	0.99643	5.70E-09
1	8	0.99415	0.99646	0.99712	0.99489	2.87E-09
1	9	0.99795	0.98925	0.99987	0.99371	2.37E-08
1	10	0.99699	0.99666	0.99661	0.99713	3.36E-09
1	20	0.99607	0.93313	0.99359	0.95614	5.85E-08
2	2	0.99456	0.99557	0.99990	0.99325	9.44E-09
2	3	0.99101	0.99691	0.99928	0.99054	1.97E-08
2	4	0.99877	0.99229	0.99956	0.99844	3.58E-09
2	5	0.99816	0.99981	0.99392	0.99788	7.31E-10
2	6	0.99820	0.99136	0.99611	0.99618	1.41E-08
2	7	0.99605	0.96847	0.96393	0.97422	5.36E-08
2	8	0.97147	0.94407	0.99873	0.41178	1.34E-07
2	9	0.99598	0.98845	0.95543	0.97974	5.09E-08
2	10	0.99682	0.99494	0.99674	0.97284	2.04E-07
2	20	0.99746	0.94327	0.96091	0.97941	9.50E-08

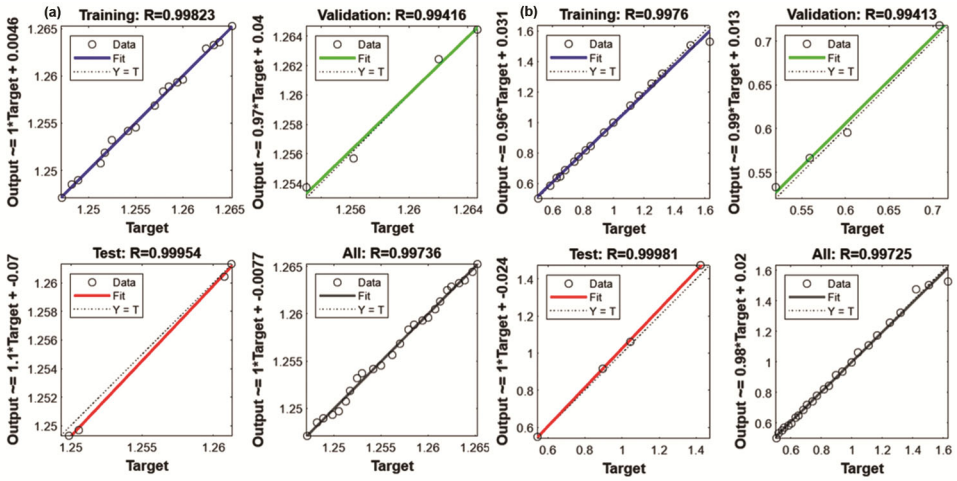

Fig. 7 — Comparison of model outputs (training, validation, testing and overall) versus experimental outputs for (a) thermal conductivity of nanofluids and (b) viscosity of nanofluids

number and have an acceptable trend and correlation coefficient. To ensure that the ANN used doesn't give rise to overfitting, the ANN is fed with test data points which are introduced for the first time. Based on the output results of the ANN model, the network of 2-6 (hidden layers - neurons per layer) is estimated to be the optimal build for modeling the thermal conductivity of hybrid nanofluid. The plot of ANN-based regression for the optimum models for thermal conductivity is given in Fig. 8(a). As for the thermal conductivity, the R^2 for the training dataset is 0.99823, whereas for validation and testing the same is 0.99416 and 0.99954, respectively, indicating a strong alignment with the datasets. The train data are forecast with appreciable accuracy with 6 neurons. The maximum MSE for the overall dataset is 2.27E-07.

From Fig. 7(a), the results have satisfactory correlational statistics to the targets because they follow the unity slope line. Similarly, for viscosity, the optimal network build is identified as 2-4 (hidden layer - neurons per layer). Fig. 7(b) gives the

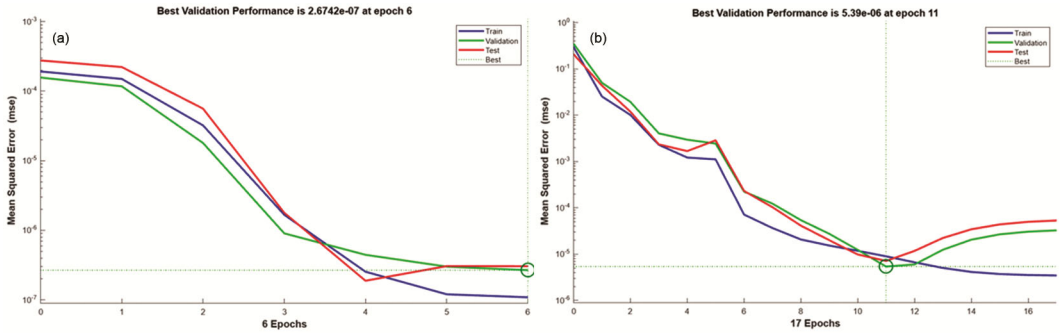

Fig. 8 — MSE vs Epochs while training neural network for (a) Thermal conductivity of nanofluids and (b) Viscosity of nanofluids

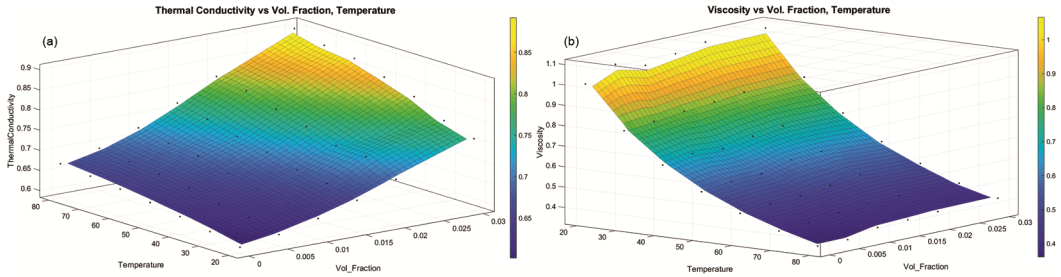

Fig. 9 — Surface Plots for (a) Thermal conductivity of nanofluids and (b) Viscosity of nanofluids

performance of the viscosity data set. The R^2 for the three datasets are 0.9976 (training), 0.99413 (validation), and 0.99981 (testing) with the overall performance being 0.99725. The model exhibits the best accuracy with 4 neurons and the maximum MSE for the overall dataset is 2.04E-07.

Another significant performance representation viz. the variation of MSE vs epoch is given in Figs 8(a) and (b) for thermal conductivity and viscosity, respectively. The standard correlation treatment by using the surface fitting method was also used in this study. The thermal conductivity and viscosity behaviour of nanofluid is predicted using a fitting method in which, φ represents the volume fraction and T represents the temperature.

The optimized correlation, along with their statistical parameters for thermal conductivity is given below in Eq. (6):

$$k(T,\phi) = 0.5788 + 1.8284\phi + 0.0011T + 100.4082\phi^2 + 0.0403\phi T \quad \ldots(6)$$

A surface is obtained (Fig. 9(a)) for the thermal conductivity by applying the polynomials for k. From the surface, it can be deduced that the thermal conductivity of the nanofluid increases with both volume fraction and temperature. Table 4 lists the statistical parameters whereas Eq. 6 indicates the fitting surface. Similarly, Eq. 7 represents the optimized correlation for the viscosity of the ternary nanofluid, and the surface is depicted in Fig. 9(b) which indicates that the viscosity of the nanofluid decreases with temperature and increases with the volume fraction.

Table 4 — Statistical parameters for the goodness of fit for thermal conductivity and viscosity at 95% CL

Parameter	Thermal Conductivity	Viscosity
SSE	0.0015	0.0104
R-square	0.9937	0.9951
Adj R-sq	0.9931	0.9944
MSE	0.0064	0.0170

$$\mu(T,\varphi) = 1.4443 - 0.0254T + 5.0336\varphi + 0.0001T^2 - 0.0144\varphi T - 71.68\varphi^2 \quad \ldots(7)$$

The statistical parameters for the goodness of fit at 95% confidence bounds are given in Table 4, which are within the desirable range. The parity plots for the thermal conductivity and viscosity correlations are given in Fig. 10(a) and (b) respectively.

From the comparison of the statistical parameters from the ANN output and the statistical fitness, it can be inferred that the ANN gives a better performance, in terms of R^2 and lower error values (MSE) compared to the correlation approach for thermal conductivity as well as viscosity. Hence the ANN treatment of data ensures better results and the cost of actual experiments can be minimized.

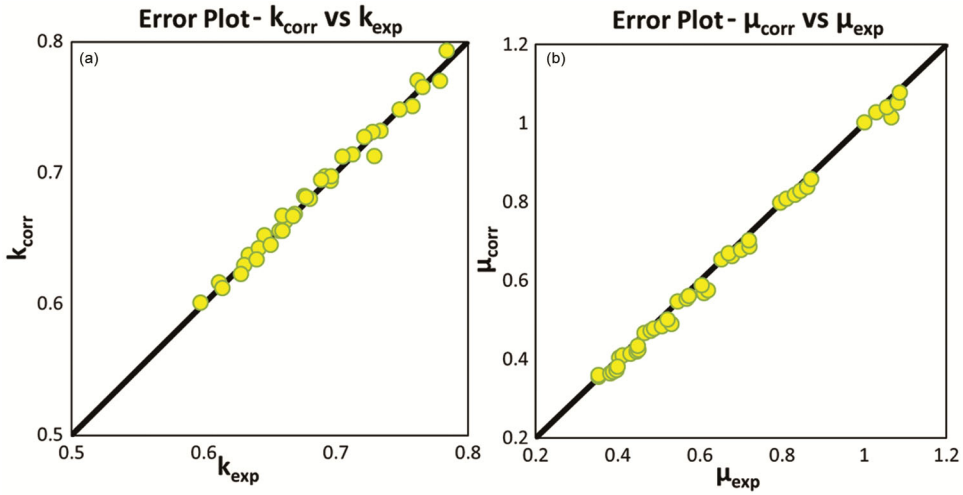

Fig. 10 — Parity Plots for (a) thermal conductivity of nanofluids and (b) viscosity of nanofluids

This study has validated the hypothesis that the ternary nanofluid containing the specific system of components will possess significantly enhanced thermophysical properties and that the selection of the LM algorithm of ANN will render better performance than the traditional fitting models. Based on the positive results obtained, the same LM-based strategy shall be applied seamlessly to model the specific heat capacity and density of the nanofluids. Also, it is proposed to study the effect of particle sizes on thermal performance and stability.

Conclusion

In this study, MWCNT-GO-Ag/water ternary hybrid nanofluid was synthesized in a two-step process followed by morphological analysis, stability determination, and estimation of thermophysical properties. The synthesized ternary nanofluid had an enhanced thermal conductivity of 0.7845 W/m.K and an appreciable viscosity of 0.8718 cP at 30°C for 3 vol %. The application of the Levenberg-Marquardt algorithm of ANN over the experimental dataset of the hybrid nanofluids resulted in the thermal conductivity and viscosity being accurately predicted using MLP feed-forward ANN analysis based on two input variables: Temperature and the solid volume fraction. The LM feed-forward network with the optimal network design of 2–6–1 (2 nodes of input layer, 6 nodes of hidden layer, and 1 node of output layer) for thermal conductivity and 2–4–1 (2 nodes of input layer, 4 nodes of hidden layer, and 1 node of output layer) for viscosity were identified as the best training approach. The ANN gave an enhanced desirable performance compared to the standard fitting technique with an overall R^2 of 0.99736 and 0.99725 for thermal conductivity and viscosity respectively. The data set employed in this study also resulted in a negligible MSE well below the surface fit. Thus, the predicted values of thermal conductivity and viscosity of MWCNT-GO-Ag/water hybrid nanofluid were found to be satisfactory and further prove the credibility of the experimental results, and the same ANN-based strategy may be applied for modeling the density and specific heat capacity parameters.

Acknowledgment

The authors acknowledge SRM Central Instrumentation Facility (SCIF), SRM Institute of Science and Technology for providing the instrumentation facilities.

Conflict of interest

The authors declare no conflict of interest.

Supplementary Information

Supplementary information is available on the website http://nopr.niscpr.res.in/handle/123456789.

References

1 Suleimanov B A, Ismailov F S & Veliyev E F, Nanofluid for enhanced oil recovery, *J Pet Sci Eng*, 78 (2011) 431.

2 Adun H, Mukhtar M, Adedeji M, Agwa T, Ibrahim K H, Bamisile O & Dagbasi M, Synthesis and application of ternary nanofluid for photovoltaic-thermal system: Comparative analysis of energy and exergy performance with single and hybrid nanofluids, *Energies*, 14 (2021) 4434.

3 Babar H & Ali H M, Towards hybrid nanofluids: Preparation, thermophysical properties, applications, and challenges, *J Mol Liq*, 281 (2019) 598.

4 Malika M, Pargaonkar A & Sonawane S S, Experimental and statistical analysis of MWCNT hybrid nanofluid-based multi-functional drilling fluid, *Chem Pap*, 77 (2023) 6773.

5 Mohammed Z J, Rasheed A K, John A, Faris W F, Aabid A, Baig M & Alallam B, Synthesis and characterization of novel ternary-hybrid nanoparticles as thermal additives, *Materials*, 16 (2023) 1.

6 Di L, Xian T, Sun X, Li H, Zhou Y, Ma J & Yang H, Facile preparation of CNT/Ag_2S nanocomposites with improved visible and NIR light photocatalytic degradation activity and their catalytic mechanism, *Micromachines*, 10 (2019) 1.

7 Keblinski P, Eastman J A & Cahill D G, Nanofluids for thermal transport, *Mater Today*, 8 (2005) 36.

8 Ahmed W, Kazi S N, Chowdhury Z Z, Johan M R B, Mehmood S, Soudagar M E M, Mujtaba M A, Gul M & Ahmad M S, Heat transfer growth of sonochemically synthesized novel mixed metal oxide ZnO+Al_2O_3+TiO_2/DW based ternary hybrid nanofluids in a square flow conduit, *Renew Sustain Energy Rev*, 145 (2021) 111025.

9 Mousavi S M, Esmaeilzadeh F & Wang X P, Effects of temperature and particles volume concentration on the thermophysical properties and the rheological behavior of CuO/MgO/TiO_2 aqueous ternary hybrid nanofluid: Experimental investigation, *J Therm Anal Calorim*, 137 (2019) 879.

10 Sharma S K B & Gupta S M, Preparation and evaluation of stable nanofluids for heat transfer application: A review, *Exp Therm Fluid Sci*, 79 (2016) 202.

11 Babu J A R, Kumar K K & Rao S S, State-of-art review on hybrid nanofluids, *Renew Sustain Energy Rev*, 77 (2017) 551.

12 Xian H W, Sidik N A C & Saidur R, Impact of different surfactants and ultrasonication time on the stability and thermophysical properties of hybrid nanofluids, *Int Commun Heat Mass Transf*, 110 (2020) 104389.

13 Zhang Y, Evans J R G & Yang S, Exploring correlations between properties using artificial neural networks, *Metall Mater Trans A Phys Metall Mater Sci*, 51 (2020) 58.

14 Srinivas T & Vinod A V, Natural convection heat transfer using water-based nanofluid in a shell and helical coil heat exchanger, *Chem Pap*, 75 (2021) 2407.

15 Borode A & Olubambi P, Modelling the effects of mixing ratio and temperature on the thermal conductivity of GNP-Alumina hybrid nanofluids: A comparison of ANN, RSM, and linear regression methods, *Heliyon*, 9 (2023) e19228.

16 El-Bakry M Y, Feed forward neural networks modeling for K-P interactions, *Chaos Solit Fractals*, 18 (2003) 995.

17 Hagan M T & Menhaj M B, Training feedforward networks with the marquardt algorithm, *IEEE Trans Neural Netw*, 5 (1994) 989.

18 Yan Z, Zhong S, Lin L & Cui Z, Adaptive levenberg-marquardt algorithm: A new optimization strategy for levenberg-marquardt neural networks, *Mathematics*, 9 (2021) 2176.

19 Sundar L S, Farooky M H, Sarada S N & Singh M K, Experimental thermal conductivity of ethylene glycol and water mixture based low volume concentration of Al_2O_3 and CuO nanofluids, *Int Commun Heat Mass Transf*, 41 (2013) 41.

20 Shaik N B, Inayat M, Benjapolakul W, Bakthavatchalam B, Barewar S D, Asdornwised W & Chaitusaney S, Artificial neural network modeling and optimization of thermophysical behavior of MXene Ionanofluids for hybrid solar photovoltaic and thermal systems, *Therm Sci Eng Prog*, 33 (2022) 101391.

21 Soltani F, Hajian M, Toghraie D, Gheisari A, Sina N & Alizadeh A, Applying Artificial Neural Networks (ANNs) for prediction of the thermal characteristics of engine oil-based nanofluids containing tungsten oxide-MWCNTs, *Case Stud Therm Eng*, 26 (2021) 101122.

22 Zhao N, Li S & Yang J, A review on nanofluids: Data-driven modeling of thermalphysical properties and the application in automotive radiator, *Renew Sustain Energy Rev*, 66 (2016) 596.

23 Naphon P, Wiriyasart S, Arisariyawong T & Nakharintr L, ANN, numerical and experimental analysis on the jet impingement nanofluids flow and heat transfer characteristics in the micro-channel heat sink, *Int J Heat Mass Transf*, 131 (2019) 329.

24 Bakthavatchalam B, Shaik N B & Hussain P B, An artificial intelligence approach to predict the thermophysical properties of MWCNT nanofluids, *Processes*, 8 (2020) 693.

25 Razavi-Dehkordi M H, Alizadeh A, Zekri H, Rasti E, Kholoud M J, Abdollahi A & Azimy H, Experimental study of thermal conductivity coefficient of GNSs-WO3/LP107160 hybrid nanofluid and development of a practical ANN modeling for estimating thermal conductivity, *Heliyon*, 9 (2023) e17539.

26 Tian S, Arshad N I, Toghraie D, Eftekhari S A & Hekmatifar M, Using perceptron feed-forward Artificial Neural Network (ANN) for predicting the thermal conductivity of graphene oxide-Al_2O_3/water-ethylene glycol hybrid nanofluid, *Case Stud Therm Eng*, 26 (2021) 101055.

27 Adun H, Kavaz D, Dagbasi M, Umar H & Wole-Osho I, An experimental investigation of thermal conductivity and dynamic viscosity of Al_2O_3-ZnO-Fe_3O_4 ternary hybrid nanofluid and development of machine learning model, *Powder Technol*, 394 (2021) 1121.

28 Ji W, Yang L, Chen Z, Mao M & Huang J N, Experimental studies and ANN predictions on the thermal properties of TiO_2-Ag hybrid nanofluids: Consideration of temperature, particle loading, ultrasonication and storage time, *Powder Technol*, 388 (2021) 212.

29 Sundar L S & Chandra M K V V, Experimental analysis and Levenberg-Marquardt artificial neural network predictions of heat transfer, friction factor, and efficiency of thermosyphon flat plate collector with MgO/water nanofluids, *Int J Therm Sci*, 194 (2023) 108555.

30 Zhang X F, Liu Z G, Shen W & Gurunathan S, Silver nanoparticles: Synthesis, characterization, properties, applications, and therapeutic approaches, *Int J Mol Sci*, 17 (2016) 1534.

31 Yu H, Zhang B, Bulin C, Li R & Xing R, High-efficient synthesis of graphene oxide based on improved hummers method, *Sci Rep*, 6 (2016) 1.

32 Zhu Y, Murali S, Cai W, Li X, Suk J W, Potts J R & Ruoff R S, Graphene and graphene oxide: Synthesis, properties, and applications, *Adv Mater*, 22 (2010) 3906.

33 Wang J, Li Y, Zheng D, Mikulčić H, Vujanović M & Sundén B, Preparation and thermophysical property analysis of nanocomposite phase change materials for energy storage, *Renew Sustain Energy Rev*, 151 (2021) 111541.

34 Plumb A P, Rowe R C, York P & Brown M, Optimisation of the predictive ability of artificial neural network (ANN) models: A comparison of three ANN programs and four classes of training algorithm, *Eur J Pharm Sci*, 25 (2005) 395.
35 Behrang M A, Assareh E, Ghanbarzadeh A & Noghrehabadi A R, The potential of different artificial neural network (ANN) techniques in daily global solar radiation modeling based on meteorological data, *Sol Energy*, 84 (2010) 1468.
36 Khan A, Khan A A P, Asiri A M & Abu-Zied B M, Green synthesis of thermally stable Ag-rGO-CNT nano composite with high sensing activity, *Compos Part B Eng*, 86 (2016) 27.
37 Xuan Y & Roetzel W, Conceptions for heat transfer correlation of nanofluids, *Int J Heat Mass Transf*, 43 (2000) 3701.
38 Sundar L S, Sharma K V, Naik M T & Singh M K, Empirical and theoretical correlations on viscosity of nanofluids: A review, *Renew Sustain Energy Rev*, 25 (2013) 670.
39 Yang L, Xu J, Du K & Zhang X, Recent developments on viscosity and thermal conductivity of nanofluids, *Powder Technol*, 317 (2017) 348.
40 Ahmadloo E & Azizi S, Prediction of thermal conductivity of various nanofluids using artificial neural network, *Int Commun Heat Mass Transf*, 74 (2016) 69.